Journal of
Mechanical
Science and
Technology

Journal of Mechanical Science and Technology 21 (2007) 1398~1407

A New Method of Controlling Cavity-induced Pressure Oscillations Using Sub-cavity

Md. Mahbubul Alam[a], Shigeru Matsuo[b,*], Kenbu Teramoto[b], Toshiaki Setoguchi[b], Heuy-Dong Kim[c]

[a]*Graduate School of Science and Engineering, Saga University, Saga 840-8502, Japan*
[b]*Department of Mechanical Engineering, Saga University, Saga 840-8502, Japan*
[c]*School of Mechanical Engineering, Andong National University, Andong, Republic of Korea*

(Manuscript Received November 17, 2006; Revised March 6, 2007; Accepted May 2, 2007)

Abstract

A new passive control technique of cavity-induced pressure oscillations has been investigated numerically for a supersonic two-dimensional flow over open rectangular cavities at Mach number 1.83 at the cavity entrance. A sub-cavity on the front wall of the cavity covered by a flat plate was evaluated for the effectiveness of controlling cavity-induced acoustic oscillations. The results showed that sub-cavity is very effective in reducing cavity-induced pressure oscillations. The results also showed that the resultant amount of attenuation of cavity-induced pressure oscillations was dependent on the length and thickness of the flat plate, and also on the depth of the sub-cavity used as an oscillation suppressor.

Keywords: Compressible flow; Supersonic cavity; Pressure oscillations; Passive control; Sub-cavity

1. Introduction

Supersonic flows of air over an open cavity can generate intense pressure oscillations that represent an important issue to be solved because of its harmful effects in many aerodynamic applications (Rossiter, 1964; Heller and Bliss, 1975; Ukeiley et al., 2004; Jeng and Payne, 1995; Rizzetta and Visbal, 2003). These intense pressure oscillations may lead to the increase of aircraft noise and drag, and may also cause severe structural vibration and fatigue of aircraft wheel wells and internal carriages of stores.

A number of passive control devices have been reported to control the cavity-induced pressure oscillations by the earlier researchers (Heller and Bliss, 1975; Ukeiley et al., 2004; Jeng and Payme, 1995; Rizzetta and Visbal, 2003). The idea of passive control technique by which cavity-induced oscillations can be reduced was first suggested by Heller and Bliss (1975). They conducted an experimental and analytical research program that studied several oscillations suppression devices such as slanting the trailing edge, upstream vortex generators or spoilers and some of those devices were able to suppress the oscillations substantially. Ukeiley et al. (2004) examined a leading-edge fence together with a cylindrical rod, placed in the oncoming boundary layer. They found that both of these devices were helpful in suppressing pressure loads in cavity flows. Jeng and Payne (1995) conducted numerical experiments to study the flowfield and suppression of pressure oscillation in open cavity at supersonic flow. They found the controlling was most effective when the rear wall of the cavity was replaced with a porous wall. Rizzetta and Visbal (2003) performed large-

*Corresponding author. Tel.: +81 952 28 8606, Fax.: +81 952 28 8587
E-mail : matsuo@me.saga-u.ac.jp

eddy simulations of supersonic cavity flowfields including active flow control through pulsed mass injection at a very high frequency. They were able to suppress the resonant acoustic oscillatory modes.

In the present numerical investigation, a passive control technique by modifying the front wall geometry of a cavity of length to depth ratio L/D = 1.0 have been studied for supersonic free stream flows. A sub-cavity on the leading edge wall of the cavity partially covered by a flat plate has been tested for the effectiveness of controlling the cavity pressure oscillations. It was found in the present study that sub-cavity is very effective in reducing cavity-induced pressure oscillations.

2. CFD analysis

2.1 Governing equations and numerical scheme

The governing equations are the unsteady compressible Navier-Stokes equations coupled with turbulence kinetic energy and eddy viscosity equations. These equations are non-dimensionalized with reference values at the inlet conditions upstream of the nozzle. A third-order TVD (Total Variation Diminishing) finite difference scheme with MUSCL (Yee, 1989) is used to discretize the spatial derivatives and a second order-central difference scheme for the viscous terms, and a second-order fractional step is employed for time integration. The turbulence model used in this simulation is a modified *k-R* model (Goldberg, 1994; Goldberg, 1996; Heiler, 1999), which is a pointwise turbulence model applicable to both wall bounded and free shear flows.

2.2 Computational domain and boundary conditions

Figure 1 shows the grids and computational domain of the cavity. The height of the main flow section above the cavity is 24 mm. The origin O in x-y coordinate is located at the leading edge of the cavity.

A cavity with aspect ratio L/D = 1.0 has been adopted for the present computational study for its two-dimensional flow structure (Sakamoto et al., 1995). The depth D and the length L of the cavity are the same and equal to 12 mm. The ratios of the length l of the flat plate to the depth of the cavity D are l/D = 0, -0.125, -0.1875 and -0.25, and the ratios of the lip thickness t to the depth of the baseline cavity D are t/D = 0.05, 0.10, 0.15, 0.20, 0.25 and 0.30. The ratios of the depth of sub-cavity d to the depth of the baseline cavity D are d/D = 0.25, 0.30, 0.35, 0.45, 0.65, 0.70 and 0.75 in the simulations. Since the static pressure distributions are the highest along the wall of aft bulkhead Jeng and Payne (1995) in comparison with that of other walls (e.g., forward bulkhead and floor) in the cavity, location of pressure measurement has been selected at (x,y) = $(L, -0.25D)$ in the present simulation. S1 in Fig.1(b) denotes the measuring position of static pressure. The number of grids is 200×80 in the region of the nozzle and 50×60 in the cavity.

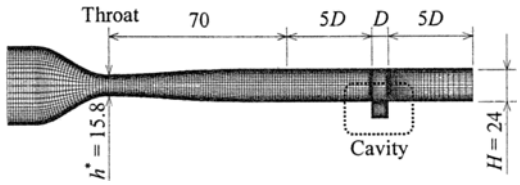

(a) Computational grids (Unit: mm)

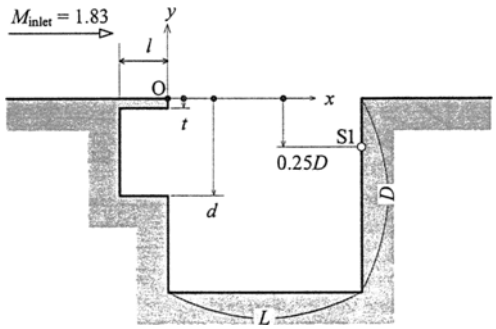

(b) Details of cavity configuration

Fig. 1. Computational domain.

In the present study, dry air is used as a working gas and assumed to be thermally and calorically perfect. Pressure p_0 in the reservoir is 101.3 kPa. The inlet Mach number M_{inlet} at the entrance of the cavity is 1.83. The Reynolds number is 2.1×10^5. On the solid walls, the no-slip conditions and no heat transfers were applied as the boundary conditions. Fixed conditions were set for the supersonic inflow boundary. Zero order extrapolation was used at the outflow boundary.

3. Results and discussion

3.1 Baseline case (cavity without control)

The validity of the computational code developed for the present numerical simulation was performed

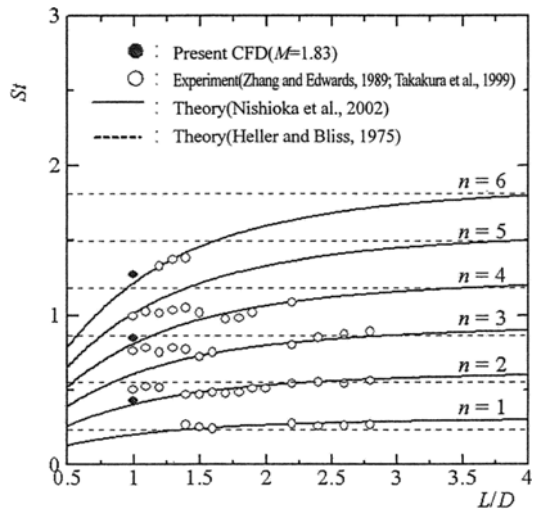

Fig. 2. Comparison of simulation results with other experimental and theoretical results.

by comparing the results of present simulation (L/D = 1.0, l/D=0, t/D=0, d/D=1.0 and M_{inlet} =1.83) with the existing results of previous researchers (Heller and Bliss, 1975; Zhang and Edwards, 1989; Takakura et al., 1999; Nishioka et al., 2002). Figure 2 shows a comparison of the Strouhal numbers St between the simulated and the experimental results (Zhang and Edwards, 1989; Takakuraet al., 1999 in Fig. 2) reported by Zhang and Edwards (1989) and Takakura et al. (1999). Closed circle represents the results of present simulation. Broken and solid lines represent the results of Heller and Bliss (1975) and Nishioka et al. (2002) respectively. The comparison shows that the simulated results are much closer to those obtained by Nishioka et al. A similar sequence of activities and the formation of typical feedback loop in the cavity were observed in the present numerical simulation that was in a good agreement with those reported by Rossiter (1964), Heller and Bliss (1975) and Nishioka et al. (2002).

Figure 3 shows contour maps of density during one period of flow oscillation for the cavity without control. Here, f represents the dominant frequency, which is equal to 17.5 kHz [see Fig. 6(a)]. It was observed that a compression wave (CW) from the trailing edge of the cavity moves upstream as time proceeds. The compression wave in Fig. 3(i) converts into an upstream traveling compression waves [CW' shown in Fig. 3(a)]. The upstream compression waves impinge on the cavity leading edge and disturb the shear layer [Fig. 3(g)]. This disturbance regenerates instability waves in the shear layer. While the shear layer reattaches at the rear wall of the cavity, generation of compression waves (CW) occurs due to the impingement of instability waves on the wall as shown in Fig. 3(a). These compression waves propagate upstream within the cavity and further

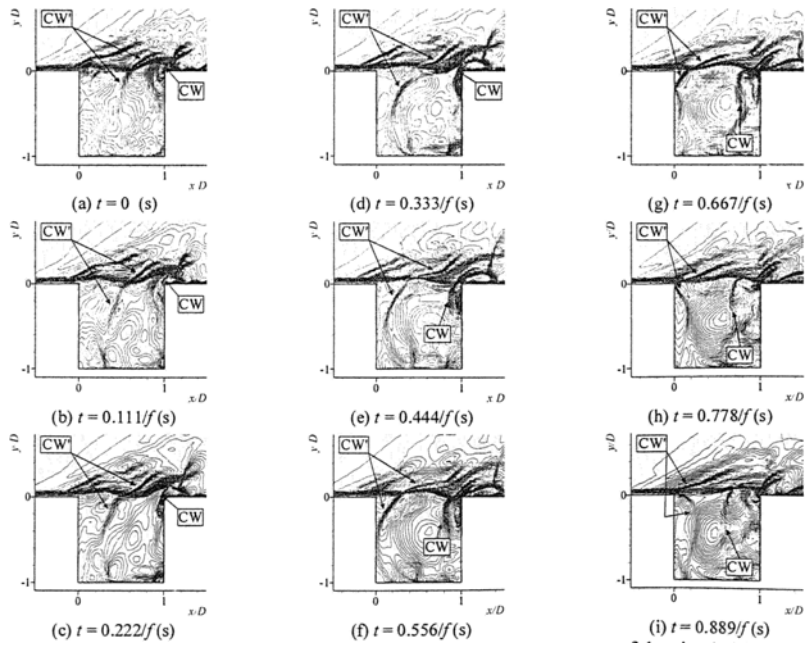

Fig. 3. Compression waves and flowfield oscillations visualized by contour maps of density (without control).

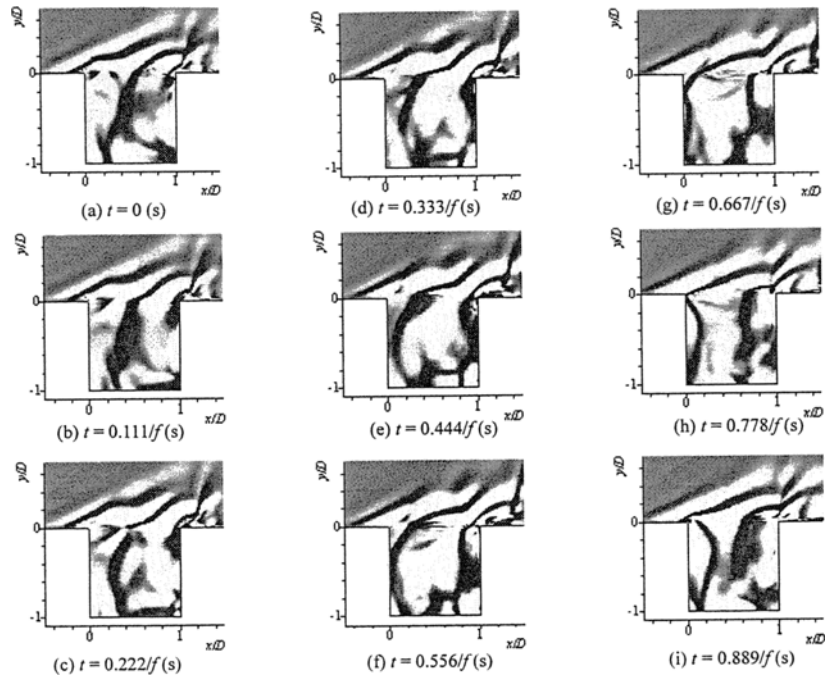

Fig. 4. Compression waves visualized by contour maps of div $\boldsymbol{u}$ in the cavity without control.

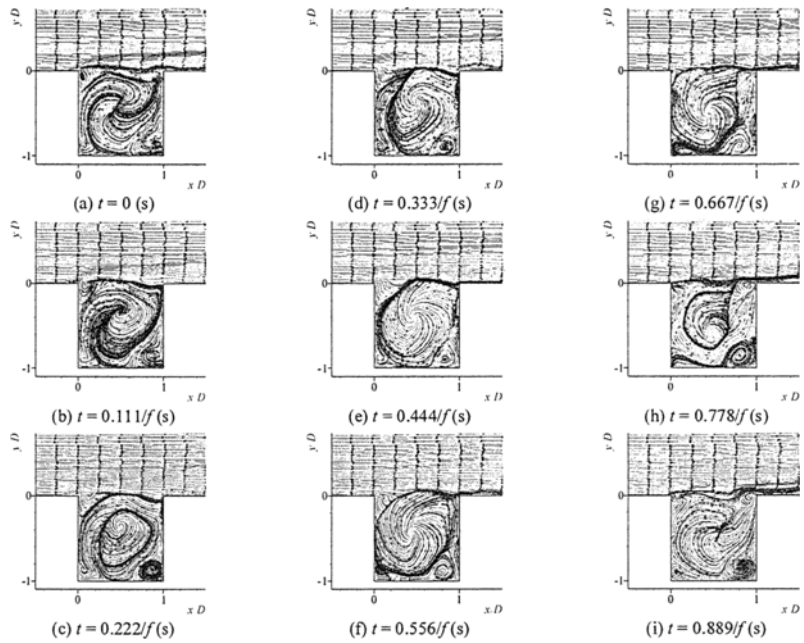

Fig. 5. Streamlines showing the flowfield oscillations (without control).

disturb the shear layer. The shear layer is continuously modified due to these subsequent disturbances and finally resonance occurs when frequency and the phase of the acoustic waves match with those of the shear layer instability waves.

Figure 4 shows the contour maps of div $\boldsymbol{u}$ for the cavity without control. This figure clearly shows the existence of compression waves because the divergence of the velocity vector $\boldsymbol{u}$ represents the change in fluid volume. The sequence of events that form the typical feedback loop, and the generation of acoustic waves at the trailing edge of the baseline cavity can also be visualized by the contour maps of div $\boldsymbol{u}$ shown in Fig. 4.

Figure 5 shows a sequence of representative instantaneous streamline contours resulting from the cavity without control. There is a very good inclination to develop a single, large vortex in the cavity accompanied by some small vortices in the corner (Roshko, 1955). Furthermore, the shedding of vortices from the leading edge corner (Quinn, 1963; Franke et al., 1975) is also observed in the cavity without control such that the vortices at the leading edge corner [Figs. 5(a) and 5(b)] are shedding on the subsequent events [Figs. 5(c) through 5(f)] increases the instability of shear layer. Figures 5(g) through 5(i) show the development of another small vortex at the leading edge corner of the cavity.

3.2 Effect of leading edge plate on the cavity flowfield

Observations were made with the introduction of the leading edge flat plate. Figure 6 shows the time histories of the static pressure at the position S1 inside the cavity with and without control. There exist large amplitudes of oscillations at this position without control as shown in Fig. 6(a). On the other hand, a substantial reduction of the amplitudes was obtained when a flat plate is introduced in the cavity (when l/D = -0.25, t/D = 0.05 and d/D = 1.0) as in Fig. 6(b). Distributions of power spectrum density at the same position obtained from the static pressure histories are shown in Fig.7. There is almost no peak frequency for case with control as shown in the Fig. 7(b) (when l/D = -0.25, t/D = 0.05 and d/D = 1.0), whereas there is a dominant frequency at 17.5 kHz in case of cavity without control [Fig. 7(a)]. It is widely believed that the feedback loop is the reason of cavity resonance that leads to increase high pressure oscillations in the cavity. Therefore, the formation of feedback loops

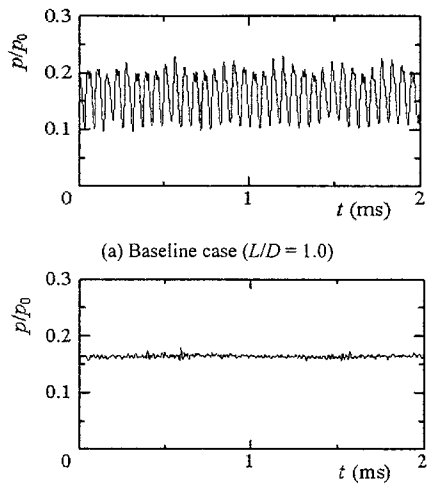

(a) Baseline case (L/D = 1.0)

(b) (l/D = -0.25, t/D = 0.05, d/D = 1.0)

Fig. 6. Time histories of static pressure.

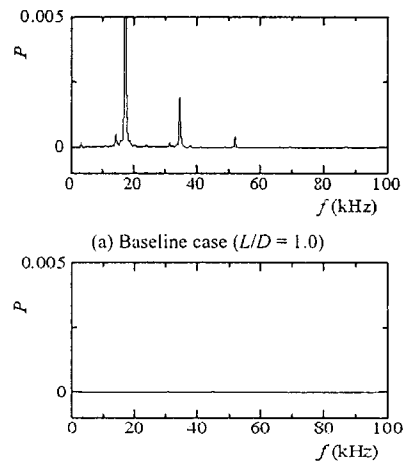

(a) Baseline case (L/D = 1.0)

(b) (l/D = -0.25, t/D = 0.05, d/D = 1.0)

Fig. 7. Distributions of power spectrum density.

and consequently the occurrence of resonance are considered to be the reason of intense pressure oscillations observed in the cavity without control as shown in Figs. 6(a) and 7(a). The significant reductions of cavity pressure oscillations that obtained by the present control device [Figs. 6(b) and 7(b)] can be explained from the fact that the upstream compression waves that impinges on the leading edge wall below the flat plate cannot disturb the shear layer immediately after the reflection. The reflected compression waves which are now below the flat plate and traveling towards downstream direction,

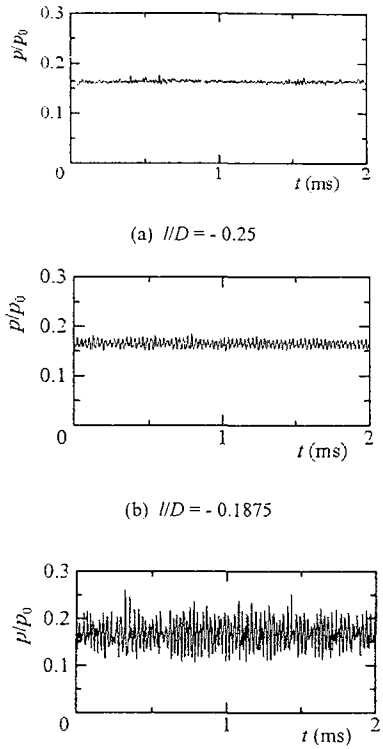

(a) l/D = - 0.25

(b) l/D = - 0.1875

(c) l/D = - 0.125

Fig. 8. Time histories of static pressure (t/D = 0.05, d/D = 1.0).

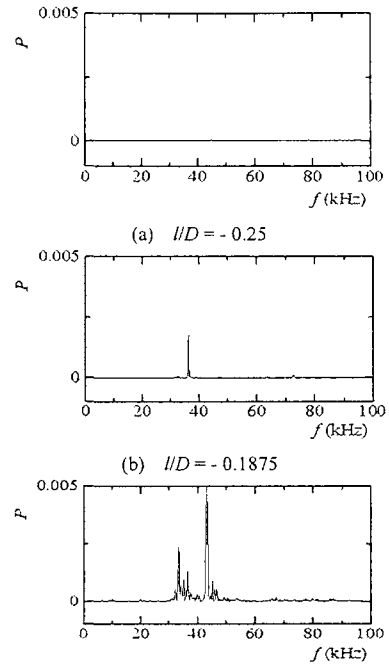

(a) l/D = - 0.25

(b) l/D = - 0.1875

(c) l/D = - 0.125

Fig. 9. Distributions of power spectrum density(t/D = 0.05, d/D = 1.0).

gradually become weaker as they travel and are to be dissipated according to Tam et al. (1996). Furthermore, Quinn (1963) and Franke and Carr (1975) showed that vortices were shed as the upstream traveling compression waves reflected from the trailing edge wall of the cavity. Therefore, interaction of the reflected compression waves with the shear layer and the shedding of vortices immediately after the reflection will not be possible in the present investigation due to the obstruction imposed by the flat plate. Furthermore, after the reflection, the gradually dissipating compression waves, while propagating towards the downstream direction, cannot excite the shear layer strongly enough to form instability waves and the formation of feedback loop is discouraged.

3.3 Effect of length of the plate

Figure 8 shows amplitudes of oscillations with different lengths of the plate at the position S1 in the cavity. The amplitude of the oscillations reduces substantially with an increase of the length of flat plate. Distributions of power spectrum density (see Fig. 9) shows that there are some peak frequencies when the length of the plate was relatively small (at l/D = -0.125 and l/D = -0.1875) and there is no peak frequency at a relatively large length of the plate (at l/D = -0.25). The reason of these results are due to the fact that the reflected compression waves which are below the flat plate have to travel more to the downstream direction in order to interact with the shear layer and become much weaker gradually with an increase of the length of the plate. Consequently, those weaker compression waves can not disturb the shear layer strongly enough to regenerate the instability waves. The best performance was obtained in case of l/D = -0.25 as shown in Figs. 8(a) and 9(a).

3.4 Effect of thickness of the plate

The effect of the plate thickness t on the flow field oscillations are shown in Fig. 10. It shows the time histories of the static pressure at the position S1 on the trailing edge of the cavity when the thickness of the plate varies. Figures 10(e) and 10(f) show very large amplitude of oscillations with larger thickness of the plate in comparison to those of Figs. 10(a) ~

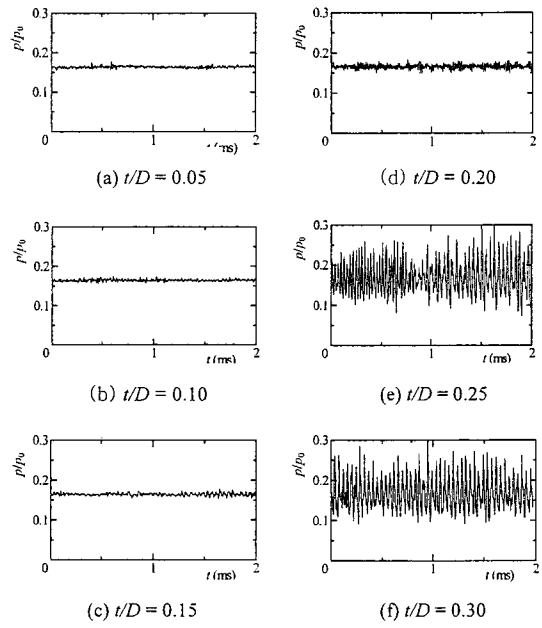

Fig. 10. Time histories of static pressure(l/D = -0.25, d/D = 1.0).

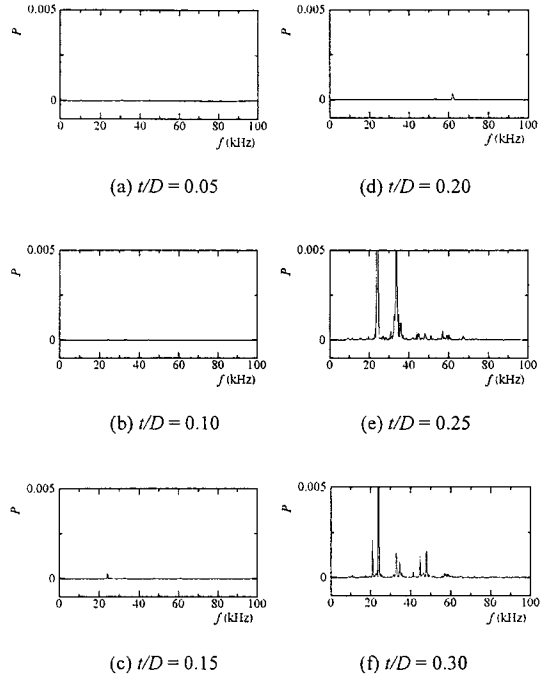

Fig. 11. Distributions of power spectrum density(l/D = -0.25, d/D = 1.0).

10(c) with smaller plate thickness. Distributions of power spectrum density (Fig. 11) also show that there is no peak frequency at a relatively small thickness of the plate and there are some strong peak frequencies at a relatively large thickness of the plate. The possibility of scattering of the upstream traveling compression waves becomes high as the thickness of the plate increases and these scattering effects help to regenerate further excitation of the shear layer and complete the feedback loop. Those investigations agreed well with that reported by several researchers (Ponton and Seiner, 1992; Raman, 1997; Jorgenson and Loh, 2002). Ponton and Seiner (1992) showed that increasing nozzle-lip thickness helped to increase maximum screech acoustic amplitudes in upstream direction. Raman (1997) described that the reflected and scattered upstream traveling acoustic waves by the larger nozzle-lip lead to a higher sound pressure level at the nozzle-lip. Jorgenson and Loh (2002) showed numerically that the thick nozzle-lip exhibited a large amount of flow entrainment, leading to a counter rotating vortex upstream of the nozzle-lip. The upstream traveling compression waves were split by the rotating entrainment vortex. A large reduction of amplitudes of oscillations was obtained with the reduction of plate thickness. Maximum reduction of the oscillations was obtained with the plate of t/D = 0.05 as shown in Fig. 10(a).

3.5 Sub-cavity as an oscillation suppressor

The results showed that the introduction of the sub-cavity together with the flat plate on the cavity front wall helped in controlling the oscillations in a favorable way such that oscillations were reduced with an increase of the depth of sub-cavity. Figure 12 shows the time histories of the static pressure at the position S1 on the trailing edge of the cavity of l/D = -0.25, t/D = 0.05 with the variation of the depth d of sub-cavity at the front wall. As seen from Figs. 12(a)~12(e), amplitudes of oscillations are larger than those in Figs. 12(f) and 12(g). Distributions of power spectrum density (see Fig. 13) also show that there is no peak frequency at a relatively higher depth of sun-cavity as in Figs. 13(f)~13(g) and there are some peak frequencies at a relatively smaller depth of sub-cavity as shown in Figs. 13(a)~13(e).

These observations can be explained by the fact that a sub-cavity at the front wall acts as an additional cavity with L/d>2 for the case shown in Figs. 12(a)~12(e). In addition to the reflections of upcoming compression waves on the cavity leading edge wall, reflections will also be occurred at the bottom face of the upper cavity. Those secondary

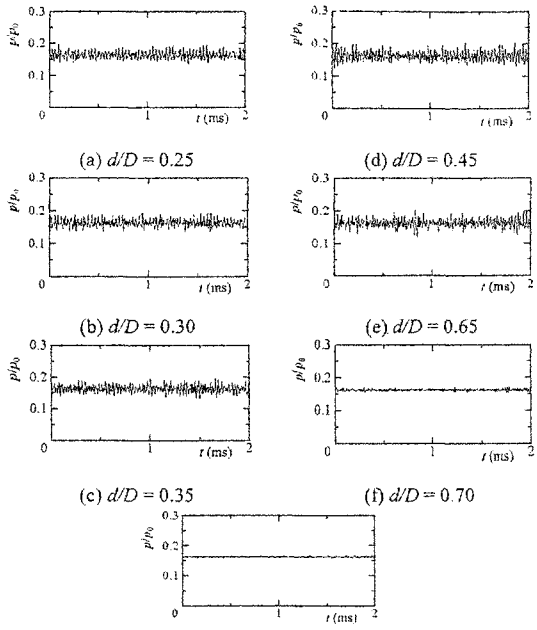

Fig. 12. Time histories of static pressure(l/D = -0.25, t/D = 0.05).

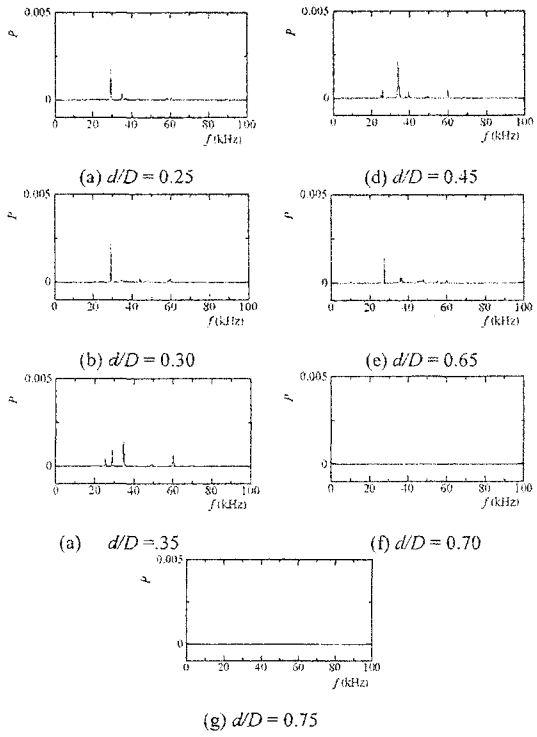

Fig. 13. Distributions of power spectrum density(l/D = -0.25, t/D = 0.05).

reflections will reach the shear layer to excite it and consequently increase the amplitude of oscillations. Increasing the depth of sub-cavity will reduce the aspect ratio of the upper cavity and the possibility of disturbances of shear layer by the secondary reflections will be reduced. According to Tam and Block (1978), for cavities with aspect ratio L/D>2, the secondary reflections of compression waves from the bottom wall of the cavity will reach the shear layer and excite it. They also described that the reflections of the upcoming compression waves from the bottom wall has an insignificant effect on the shear layer instability for a cavity with L/D<2. The result of the present simulation agrees well with that reported by Tam and Block.

Figure 14 shows typical density contours for the cavity without control. There exist no upstream compression waves or the reflected waves as shown in Figs. 14(a) through 14(i). As it is explained in Sec. 3.2, the reflected compression waves cannot disturb the shear layer strongly enough to increase the instability due to the leading edge plate. Furthermore, the instability of shear layer is not strong enough to produce compression waves. Therefore, there exists a stable shear layer in the cavity with control.

Figure 15 shows the streamlines of flowfield with control (l/D = -0.25, t/D = 0.05 and d/D = 0.75). There exists a large, single and stable vortex in the main cavity. Figure 15 also shows that in the sub-cavity there is developing another large vortex which is obstructed by the leading edge plate. Therefore, shedding of small vortices which disturbs the shear layer is discouraged here in the cavity with control and there exists a stable shear layer.

4. Concluding remarks

Computational investigation has been carried out for a supersonic two-dimensional flow over open, square cavities at Mach number 1.83 at the cavity entrance. A sub-cavity on the front wall of the cavity with a flat plate had been investigated for the effectiveness of controlling cavity pressure oscillations. The results showed that the length and thickness of the flat plate had a great influence in controlling the cavity-induced acoustic oscillations. The amplitudes of the oscillations were reduced substantially with an increased of the length of the flat plate. Furthermore, a decrease in the plate thickness also assisted to suppress the oscillations remarkably.

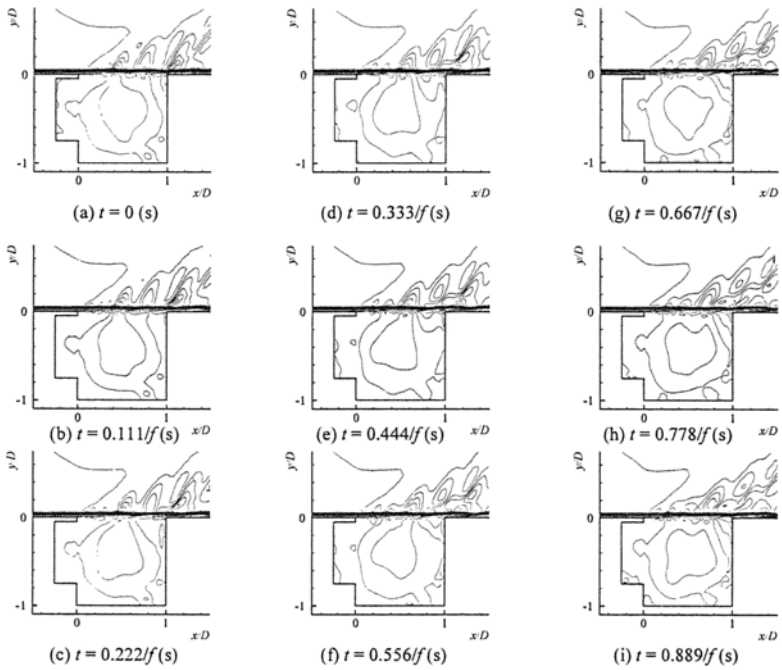

Fig. 14. Contour maps of density showing flowfield oscillations (with control).

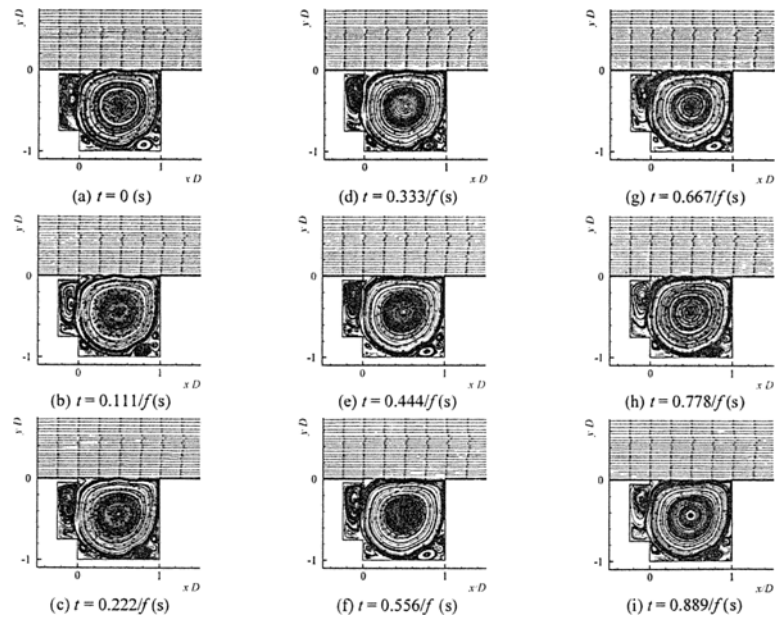

Fig. 15. Streamline showing the flowfield with control(D = -0.25, t/D = 0.05, d/D = 0.75).

The results also showed that the resultant amount of attenuation of cavity-induced acoustic oscillations was dependent on the depth of the sub-cavity.

Nomenclature

f : Frequency, Hz
l : Plate length, m
L : Cavity length, m
M : Mach number, -
n : Mode number, -
p : Pressure, Pa
St : Strouhal number, -
t : Time, sec
t : Plate thickness, m
d : Depth of sub-cavity, m
u : Cartesian velocity component, m/s
x,y : Cartesian coordinates, m

Subscripts

0 : Stagnation

Acknowledgement

This work was financially supported by the Japan Science Society through the Sasagawa Scientific Research Grant (No. 18-056).

References

Franke, M.E., Carr, D.L., 1975, "Effect of Geometry on Open Cavity Flow-Induced Pressure Oscillations," *AIAA*, pp. 75~492.

Goldberg, U. C., 1994, "Toward a Pointwise Turbulence Model for Wall-Bounded and Free Shear Flows," *Transactions of the ASME*, Vol. 116.

Goldberg, U. C., 1996, "Exploring a Three-Equation $R-k-\varepsilon$ Turbulence Model," *Journal of Fluids Engineering*, Vol. 118.

Heiler, M., 1999, "Instationäre Phänomene in Homogen/Heterogen Kondensierenden Düsenund Turbinenströmungen, Dissertation," *Fakultät für Maschinenbau*, Universität Karlsruhe, Germany.

Heller, H. H., and Bliss, D. B., 1975, "The Physical Mechanism of Flow-induced Pressure Fluctuations in Cavities and Concepts for their Suppression," *AIAA*, pp. 75-491, AIAA Aero-Acoustics Conf.

Jeng, Y. N., Payne, U. J., 1995, "Numerical Study of a Supersonic Open Cavity Flow and Pressure Oscillation Control," *Journal of Aircraft*, Vol. 32-2.

Jorgenson, P. C. E., Loh, C. Y., 2002, "Computing Axisymmetric Jet Screech Tones Using Unstructured Grids," *AIAA*, pp. 2002-3889.

Nishioka, M, Asai, T., Sakaue, S., Shirai, K., 2002, "Some Thoughts on the Mechanism of Supersonic Cavity Flow Oscillation, Part 2 A New Formula for the Oscillation Frequency," *Journal of Japan Society of Fluid Mechanics*, Vol.21.

Ponton, M.K., Seiner, J.M., 1992, "The Effects of Nozzle Exit Lip Thickness on Plume Resonance." *Journal of Sound and Vibration*, Vol. 154-3.

Quinn, B., 1963, "Flow in the Orifice of a Resonant Cavity," *AIAA Student Journal*, Vol. 1.

Raman, G., 1997, "Cessation of Screech in Underexpanded Jets," *Journal of Fluid Mechanics*, Vol. 336.

Rizzetta, D. P. and Visbal, M. R., 2003, "Large-eddy Simulation of Supersonic Cavity Flowfields Including Flow Control," *AIAA Journal*, Vol. 41-8.

Roshko, A., 1955, "Some Measurements of Flow in a Rectangular Cutout," NACA TN-3488.

Rossiter, J. E., 1964, "Wind-Tunnel Experiments on the Flow over Rectangular Cavities at Subsonic and Transonic Speeds," *Aeronautical Research Council Reports and Memoranda*, No. 3438.

Sakamoto, K., Matsunaga, K., Fujii, K., Tamura, Y., 1995, "Experimental Investigation of Supersonic Internal Cavity Flows," *AIAA*, pp. 95~2213.

Takakura, Y., Suzuki, T., Higashino, F., Yoshida, M., 1999, "Numerical Study on Supersonic Internal Cavity Flows: What Causes the Pressure Fluctuations?," *AIAA*, pp. 99~0545.

Tam, C. J., Orkwis, P. D., Disimile, P. J., 1996, "Algebraic Turbulence Model Simulations of Supersonic Open-Cavity Flow Physics," *AIAA Journal*, Vol. 34.

Tam, C. K. W., Block, P. J. W., 1978, "On the Tones and Pressure Oscillations Induced by Flow over Rectangular Cavities," *Journal of Fluid Mechanics*, Vol. 89.

Ukeiley, L. S., Ponton, M. K., Seiner, J. M. and Jansen, B., 2004, "Suppression of Pressure Loads in Cavity Flows," *AIAA Journal*, Vol. 42, No. 1.

Yee, H. C., 1989, "A Class of High-resolution Explicit and Implicit Shock Capturing Methods," NASA TM-89464.

Zhang, X., Edwards, J. A., 1989, "An Investigation of Supersonic Oscillatory Cavity Flows Driven by Thick Shear," *Aeronautical Journal*, pp. 355~364.